5378 *Macromolecules* **2009**, *42*, 5378–5387
DOI: 10.1021/ma9003049

Macromolecules
ARTICLE

Dynamics of Semiflexible Chains, Stars, and Dendrimers

Maxim Dolgushev* and Alexander Blumen

Theoretical Polymer Physics, University of Freiburg, Hermann-Herder-Strasse 3, D-79104 Freiburg, Germany

Received February 10, 2009; Revised Manuscript Received May 11, 2009

ABSTRACT: Focusing on mechanical and dielectric relaxation, we study the dynamics of semiflexible linear chains, stars, and dendrimers. For this, we use an extension of the Rouse-model in which we include, in the spirit of Bixon and Zwanzig (*J. Chem. Phys.* **1978**, *68*, 1896) and of von Ferber and Blumen (*J. Chem. Phys.* **2002**, *116*, 8616), restrictions on the bonds' orientations. In every case the dynamical matrix in the bonds' representation turns out to be a sparse matrix, a fact which simplifies its diagonalization and may pave the way for further analytical treatments.

Introduction

Recently, based on the classical Rouse−Zimm approach[1,2] much effort has been invested in the evaluation of the dynamical properties of extremely large polymer structures.[3] While Rouse−Zimm models neglect a whole series of basic features (such as the excluded volume, the stiffness of the structures and the entanglements), they allow to display aspects typical of the underlying topology, aspects which appear only when very large systems are considered.[3,4] Especially the Rouse variant has turned out to be particularly fruitful; its extension to the concept of generalized Gaussian structures (GGS) has allowed a semianalytical treatment of dendrimers,[5−8] of regular hyperbranched fractals[9,10] and of fractal structures with loops.[4,11−13] In these cases, by a judicious assessment of the underlying symmetry, one succeeded in establishing the form of the eigenvectors and in factorizing the characteristic polynomial of the Langevin matrix involved, sometimes to such a level that its eigenvalues could be determined very precisely through iterative procedures.[4−6,9,10] Fundamental in this respect is the sparsity (the fact that most of the entries vanish) of the matrices under study.[14]

In the present work we will implement stiffness into the Rouse-model, in the spirit of the approach by Bixon and Zwanzig (BZ).[15] The BZ-approach for semiflexible chains is very fruitful and of steady interest; new advances are summarized in ref 16. Recently an extension of the BZ-model was used in the study of melts of polymer chains.[17] Another variant of the model has been proposed in order to describe protein dynamics.[18] The basic idea of introducing stiffness, as exemplified in ref 15 for linear chains, consists in viewing the bonds between consecutive Rouse beads as oriented vectors and in fixing the average value of the angle between them. The idea is readily extended to branched structures by appropriate restrictions,[7,15,19−21] also vide infra. Clearly, such an approach, originally called optimized Rouse−Zimm model,[15] presupposes a discrete object and differs from models in which the polymer chain segments are taken to be continuous, such as in the wormlike chain model (WLC).[22−25]

An interesting aspect to note is that most of the works devoted to discrete semiflexible polymers have chosen to stay within the optimized Rouse−Zimm framework, by taking both the hydrodynamic interactions and the stiffness parameters into account.[19−21] As we proceed to show, this choice (while somehow more realistic) generally leads to Langevin equations whose matrices are rather complex and which do not show sparsity. Here we will follow a different course: We will stay within the Rouse scheme of the GGS, while including the stiffness between the bonds of the model polymer.[7] As we proceed to show, not only for linear chains but also for stars and for dendrimers, the procedure leads to sparse matrices in the bonds' representation. On the basis of this knowledge, the calculation of the dynamical characteristics simplifies drastically, fact which allows us to compute the mechanical and dielectric relaxation forms for large structures.

The form of the present paper is as follows: In the next section, we summarize the basis of the GGS and introduce the relations that allow to take semiflexibility into account. In the section Examples, we recall the classical findings for linear chains and derive in analytical form the corresponding sparse matrices also for star polymers and for dendrimers. In the section Dynamics we derive the form of the complex dielectric susceptibility for semiflexible, type A polymers in Stockmayers' classification[26] and recall the forms of the storage and of the loss moduli. Then, in the following section, we display our results for semiflexible star polymers and dendrimers, in which we use both the formulas and the eigenvalues and eigenvectors which we derived. In the last section, we close with Conclusions.

Theory

Starting in the framework of generalized Gaussian structures (GGS),[3] we study here tree-like networks, which include, in particular, linear chains, stars, and dendrimers. The GGS are an extension of the classical Rouse approach for linear chains,[1] in which the vertices are the beads (monomers) and the bonds (segments) are the springs. The configuration of a GGS is given by the set of position vectors of the N monomers $\{\mathbf{r}_i\}$, where $\mathbf{r}_i(t)$ is the position vector of the ith bead at time t. We focus on tree-like networks only, so that the N beads are connected by $N-1$ bonds. We denote these bonds by $\{\mathbf{d}_a\}$ ($a = 1, \ldots, N-1$), so that the "a" bond is related to the beads "i" and "j" which it connects, through

$$\mathbf{d}_a = \mathbf{r}_j - \mathbf{r}_i \tag{1}$$

This relation can be formulated in matrix form by introducing the matrices $\mathbf{D}_\alpha$ and $\mathbf{R}_\alpha$ as the columns of the $\alpha = \{x,y,z\}$ components of the bond vectors $\{\mathbf{d}_a\}$ and the position vectors $\{\mathbf{r}_i\}$,

*Corresponding author. E-mail: dolgushev@physik.uni-freiburg.de.

 Published on Web 06/17/2009

respectively. From eq 1, it follows that

$$\mathbf{D}_\alpha = \mathbf{P}\mathbf{R}_\alpha \tag{2}$$

For each bond $\mathbf{d}_a$ that is directed from bead i to bead j the $(N-1)\times N$ matrix $\mathbf{P} \equiv (P_{ai})$ has as nonzero entries only $P_{ai} = -1$ and $P_{aj} = 1$. In the mathematical literature,[27] the transposed matrix $\mathbf{P}^T$ is well-known as the incidence matrix $\mathbf{G} \equiv (G_{ia})$; therefore, eq 2 takes the form

$$\mathbf{D}_\alpha = \mathbf{G}^T\mathbf{R}_\alpha \tag{3}$$

The dynamics of a polymeric structure is described in the Rouse-scheme by the Langevin equation:

$$\zeta\frac{\partial}{\partial t}r_{\alpha i}(t) + \frac{\partial}{\partial r_{\alpha i}}V_R(\{\mathbf{r}_k\}) = f_{\alpha i}(t) \tag{4}$$

Here α runs over the components x, y, and z, ζ is the friction coefficient, $f_{\alpha i}(t)$ is the α component of the usual Gaussian random force acting on the ith bead for which $\langle \mathbf{f}_k(t)\rangle = 0$ and $\langle f_{\alpha k}(t) f_{\beta m}(t')\rangle = 2k_BT\zeta\delta_{km}\delta_{\alpha\beta}\delta(t-t')$ holds, and $V_R(\{\mathbf{r}_k\})$ is the harmonic potential

$$V_R(\{\mathbf{r}_k\}) = \frac{K}{2}\sum_{\alpha,m,n} r_{\alpha m}A^R_{mn}r_{\alpha n} \tag{5}$$

In eq 5, all bonds have been taken to be equal, with spring constant $K = 3k_BT/l^2$, where l^2 is the mean-square length of each bond and k_B is the Boltzmann constant. The $N\times N$ matrix $\mathbf{A}^R \equiv (A^R_{ij})$ is the connectivity matrix and is symmetric. Each diagonal element A^R_{ii} equals the number of bonds emanating from ith bead, and the off-diagonal elements of $\mathbf{A}^R$ are either -1 if i and j are connected by a bond, or 0 otherwise.

With the potential $V_R(\{\mathbf{r}_k\})$ given by eq 5, the Langevin equation decouples in terms of the components x, y, and z. Therefore one has for each α-component in matrix form:

$$\zeta\frac{\partial \mathbf{R}_\alpha(t)}{\partial t} + K\mathbf{A}^R\mathbf{R}_\alpha(t) = \mathbf{F}_\alpha(t) \tag{6}$$

Here $\mathbf{F}_\alpha$ is the column of the α-components of the Langevin random forces $\{f_{\alpha i}\}$.

The Rouse connectivity matrix $\mathbf{A}^R$ is related to the incidence matrix $\mathbf{G}$ by the expression[27]

$$\mathbf{A}^R = \mathbf{G}\mathbf{G}^T \tag{7}$$

as is easy to verify as follows: $(\mathbf{G}\mathbf{G}^T)_{ij}$ is the inner product of the rows i and j of $\mathbf{G}$. If $i \neq j$, then these rows have a nonzero entry in the same column a if and only if there is a bond a joining the beads i and j. In this case, the two nonzero entries are $+1$ and -1, so that $(\mathbf{G}\mathbf{G}^T)_{ij} = -1$. Similarly, $(\mathbf{G}\mathbf{G}^T)_{ii}$ is the inner product of the row i with itself, and, since the number of entries (which can be $+1$ or -1) in the ith row is equal to the functionality f_i of the ith bead, this results in $(\mathbf{G}\mathbf{G}^T)_{ii} = f_i$. Hence $\mathbf{G}\mathbf{G}^T$ reproduces the definition of the connectivity matrix $\mathbf{A}^R$. Replacing now in eq 5 $\mathbf{A}^R$ by $\mathbf{G}\mathbf{G}^T$ and using twice eq 3 leads to:

$$V_R(\{\mathbf{d}_a\}) = \frac{K}{2}\sum_\alpha \mathbf{D}^T_\alpha\mathbf{D}_\alpha = \frac{K}{2}\sum_a \mathbf{d}_a{}^2 \tag{8}$$

This relation recovers the physically obvious fact that in the bonds' representation the potential eq 5 has a diagonal form.

Now, semiflexibility can be introduced in GGS scheme by inserting geometrical restrictions on the bonds' orientations. Originally[15] this was done in the framework of generalized Langevin equations;[28] equivalently, one can implement semiflexibility by generalizing eq 8 and taking[7]

$$V_{BZ}(\{\mathbf{d}_a\}) = \frac{K}{2}\sum_{a,b} W_{ab}\mathbf{d}_a\cdot\mathbf{d}_b \tag{9}$$

The general form of the potential V_{BZ}, eq 9, allows to impose restrictions on the angles between the bonds of the GGS through the matrix $\mathbf{W} \equiv (W_{ab})$. Namely, calculating the equilibrium bond−bond correlations $\langle \mathbf{d}_a\cdot\mathbf{d}_b\rangle$ with respect to the Boltzmann distribution $\exp(-V_{BZ}/k_BT)$ yields, under the assumption that the $\{\mathbf{d}_a\}$ are Gaussian

$$\langle \mathbf{d}_a\cdot\mathbf{d}_b\rangle = l^2(\mathbf{W}^{-1})_{ab} \tag{10}$$

Clearly, there are different ways in which the matrix $\mathbf{W}$ could be built. However if we take for $\mathbf{W}$ the inverse of the matrix $\mathbf{V} \equiv (V_{ab})$ constructed according to the physically plausible conditions listed below, then it turns out for several systems of basic importance (such as linear chains, stars and dendrimers) that the corresponding matrices $\mathbf{W}$ have a particular and sparse form.

Here is the list of rules which allow to define the matrix $\mathbf{V}$ by stipulating conditions on the $\{V_{ab}\}$. First

$$V_{aa} = 1 \tag{11}$$

a relation reflecting the fact that the mean-squared bond length is fixed, $\langle \mathbf{d}_a\cdot\mathbf{d}_a\rangle = l^2$. Second, for adjacent bonds a and b connected by the common bead i, stiffness is introduced through the condition

$$V_{ab} = \pm t_i \tag{12}$$

In eq 12 the parameter t_i depends on i (see the discussion below) and the bonds are directed so that the plus sign is chosen for a head to tail arrangement, whereas the minus sign appears in the two other cases. Third, for a tree-like network all nonadjacent bonds, e.g., a and c, are connected by a unique shortest path (b_1, b_2,...,b_{k-1},b_k), where a is adjacent to b_1, b_i to b_{i+1} and b_k to c. Thus, in the spirit of the freely rotating chain model, we assume the following relation to hold:

$$V_{ac} = V_{ab_1}V_{b_1b_2}\ldots V_{b_kc} \tag{13}$$

Let us now focus on the possible values which the t_i may reasonably take. As we will proceed to show, this range depends on the functionality f_i of i, so that t_i lies between 0 and $1/(f_i-1)$. First, in the case that all correlations between the orientations of different bonds vanish, we have a fully flexible polymer. Now this corresponds to having $t_i = 0$ for all i. It is now a simple matter to verify that, following eqs 12 and 13, $\mathbf{V}$ is the unit matrix, and so is then $\mathbf{V}^{-1}$, i.e. $\mathbf{W}$. By this eq 9 turns into eq 8. Second, we take a fixed, rigid configuration of bonds around i, orient them pointing away from i and denote by θ_{ab} the angle between a and b. Now, as before, $<\cos\theta_{ab}> = -t_i$, where we took the tail to tail configuration into account. On the other hand, in three dimensions, the sum of the cosines of all pairs of angles is bounded[29] by $\sum_{a<b}\cos\theta_{ab} \geq -f_i/2$. Since the number of pairs of bonds is $f_i(f_i-1)/2$, it follows by averaging that $-t_i(f_i-1) \geq -1$, i.e., that

$$t_i \leq 1/(f_i-1) \tag{14}$$

Whether now situations exist in which $t_i = 1/(f_i-1)$ and all angles between bonds are exactly equal depends on f_i and on the embedding space. The question is simple for $f_i = 2$ and dimensions equal or larger than 1, where one is led to stiff rods; in fact,

in the BZ-picture one obtains in this limit so-called Gaussian rods, as discussed in ref 30. Now for $f_i = 3$ one has $t_i = {}^1/_2$ for a planar arrangement, with an angle of $2\pi/3$ between the bonds; for $f_i = 4$ one needs a 3-dimensional space in order to have an arrangement in which all 6 pairs of bonds involved are equal, with $\cos\theta = -1/3$, the structure being a tetrahedron; the strict equality of *all* mutual angles cannot be realized anymore for $f_i \geq 5$ in three dimensions. Evidently, for any $f_i \geq 4$, there are many realizations of $\sum_{a<b} \cos\theta_{ab} \geq -f_i/2$ possible, if one discards the condition of the strict equality of *all* angles.

Examples

In this section, we consider linear chains, stars, and dendrimers. For all listed examples we provide the matrix **V**. Then we display its inverse, $\mathbf{W} = \mathbf{V}^{-1}$, and prove that indeed $\mathbf{VW} = \mathbf{1}$, where **1** is the unit matrix.

Linear Chains. In this section we recall the well-known forms[15] for **V** and for **W** for a linear chain of N beads. Figure 1 displays such a chain, in which the bond vectors are arranged head to tail. For simplicity we assume all the t_i to be equal, $t_i \equiv t$ for all i, and, as discussed above, take $t < 1$. Using eqs 11, 12, and 13, **V** reads:

$$\mathbf{V} = \begin{pmatrix} 1 & t & \dots & t^{N-3} & t^{N-2} \\ t & 1 & \dots & t^{N-4} & t^{N-3} \\ t^2 & t & \ddots & \vdots & \vdots \\ \vdots & \vdots & \dots & 1 & t \\ t^{N-2} & t^{N-3} & \dots & t & 1 \end{pmatrix} \tag{15}$$

As we proceed to show, for $t < 1$, the matrix **V** has an inverse. Consider namely

$$\mathbf{W} = \frac{1}{1-t^2} \begin{pmatrix} 1 & -t & 0 & \dots & 0 \\ -t & 1-t^2 & -t & \ddots & \vdots \\ 0 & \ddots & \ddots & \ddots & 0 \\ \vdots & \ddots & -t & 1-t^2 & -t \\ 0 & \dots & 0 & -t & 1 \end{pmatrix} \tag{16}$$

We first note the structure of **W**: it is a sparse matrix with particular features; the diagonal elements corresponding to internal bonds equal $(1 + t^2)/(1 - t^2)$, whereas those corresponding to peripheral bonds equal $1/(1 - t^2)$. The matrix elements next to the diagonal elements equal $-t/(1 - t^2)$, whereas the matrix elements corresponding to bonds without a common site vanish. As we will show in the following, such regularities also show up in the more complex cases considered below. We note that the sparsity of **W** is also a key point in obtaining the memory functions for the segments' orientations in linear chains.[31]

It is now a simple matter to verify that indeed $\mathbf{VW} = \mathbf{1}$ holds, by directly multiplying eqs 15 and 16. We note that **W** for linear chains was already given by Bixon and Zwanzig[15] and that this expression is also a consequence of the maximum entropy principle in the treatment of stiffness used by Winkler, Reineker, and Harnau.[25,32]

Star Polymers. As next example we focus on star polymers consisting of f arms and having n bonds in each arm. In Figure 2, we display such a star for which the functionality of the central bead (core) is $f = 3$ and all bonds have their orientations pointing away from the core. We number the bonds consecutively along each of the arms of the star, having hence $(\mathbf{d}_1,\dots,\mathbf{d}_n)$ for the first arm, $(\mathbf{d}_{n+1},\dots,\mathbf{d}_{2n})$ for the second one, etc., as also indicated in Figure 2. We set q for the stiffness parameter of the bonds associated with the core, $q < 1/(f - 1)$, and t with $t < 1$ for all other stiffness parameters.

Figure 1. Bonds of a chain molecule consisting of N beads. The configuration of the segments is head to tail and they are numbered from left to right in ascending order.

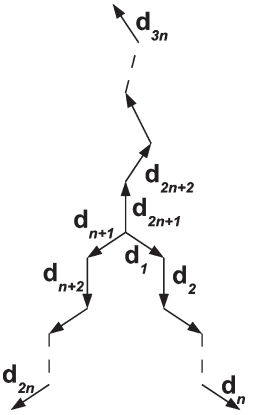

Figure 2. Bonds of a star molecule whose central bead has functionality $f = 3$. See the text for details.

According to eqs 11, 12, and 13, the matrix **V** has now the following block form:

$$\mathbf{V} = \begin{pmatrix} \mathbf{T} & \mathbf{S} & \dots & \mathbf{S} \\ \mathbf{S} & \ddots & \ddots & \vdots \\ \vdots & \ddots & \ddots & \mathbf{S} \\ \mathbf{S} & \dots & \mathbf{S} & \mathbf{T} \end{pmatrix} \tag{17}$$

Namely, **V** consists of $f \times f$ block matrices, each of which is a $n \times n$ matrix. The elements of the matrices $\mathbf{T} = (T_{ij})$ on the main diagonal are given, as in the previous case, by $T_{ij} = t^{|i-j|}$, where i and j run from 1 to n. The elements of the off-diagonal matrices $\mathbf{S} = (S_{ij})$ (where again i and j run from 1 to n) are given by $S_{ij} = -qt^{(i+j-2)}$. One can note here that the shortest path connecting two bonds on distinct arms of the chain passes through the core (which leads to the factor q) and that then one change of direction occurs, hence giving the factor (-1).

We now claim that the **W** matrix corresponding to the matrix **V** of eq 17 has the following form:

$$\mathbf{W} = \begin{pmatrix} \mathbf{W}_1 & \mathbf{W}_2 & \dots & \mathbf{W}_2 \\ \mathbf{W}_2 & \ddots & \ddots & \vdots \\ \vdots & \ddots & \ddots & \mathbf{W}_2 \\ \mathbf{W}_2 & \dots & \mathbf{W}_2 & \mathbf{W}_1 \end{pmatrix} \tag{18}$$

Hence, the matrix **W** also consists of $f \times f$ blocks, each of the form $n \times n$. The diagonal blocks $\mathbf{W}_1$ of **W** have the following structure:

$$\mathbf{W}_1 = \begin{pmatrix} \lambda_c & \mu & 0 & \dots & 0 \\ \mu & \lambda & \mu & \ddots & \vdots \\ 0 & \ddots & \ddots & \ddots & 0 \\ \vdots & \ddots & \mu & \lambda & \mu \\ 0 & \dots & 0 & \mu & \lambda_p \end{pmatrix} \tag{19}$$

Here the off-diagonal blocks $\mathbf{W}_2$ contain only one nonzero element μ_c; their structure is

$$\mathbf{W}_2 = \begin{pmatrix} \mu_c & \dots & 0 \\ \vdots & \dots & \vdots \\ 0 & \dots & 0 \end{pmatrix} \tag{20}$$

Moreover, the parameters appearing in eqs 19 and 20 are (as a function of t and q) as follows:

$$\lambda = (1 + t^2)/(1-t^2) \tag{21}$$

$$\lambda_c = 1/(1-t^2) + (f-1)q^2/((1+q)(1-(f-1)q)) \tag{22}$$

$$\lambda_p = 1/(1-t^2) \tag{23}$$

$$\mu = -t/(1-t^2) \tag{24}$$

$$\mu_c = q/((1+q)(1-(f-1)q)) \tag{25}$$

One can again remark that **W** is sparse, that the matrix elements corresponding to pairs of bonds without a common site vanish and that in **W** five constants show up, depending on whether the bonds are peripheral, connected to the core (central) or otherwise internal (interarm), and whether adjacent bonds are connected through the core or through another site.

We now show that for **V** and **W** given by eq 17 and eq 18, respectively, we indeed have **VW** = **1**. We start by setting **K** = **VW** and show step-by-step that **K** = **1**. With each element of the matrix **K** = (k_{ab}) are associated the bond vectors $\mathbf{d}_a$ and $\mathbf{d}_b$. Now each bond vector, e.g., $\mathbf{d}_b$, can be either central ($b \in (1, n+1,\ldots,(f-1)n+1)$) or peripheral ($b \in (n,2n,\ldots,fn)$) or interarm. In all these cases we consider first the diagonal elements and the elements associated with bonds adjacent to $\mathbf{d}_b$, doing it columnwise. Thereafter we consider the elements corresponding to nonadjacent bonds.

Let us begin with $\mathbf{d}_b$ being central. For the element k_{ab}, associated with $\mathbf{d}_b$ and any other central $\mathbf{d}_a$, we have from eqs 17 to 20:

$$k_{ab} = -q\lambda_c - qt\mu + [1-(f-2)q]\mu_c \tag{26}$$

Together with eqs 21−25, it follows that

$$k_{ab} = 0 \tag{27}$$

The diagonal element k_{bb} associated with the vector $\mathbf{d}_b$ is given by

$$k_{bb} = \lambda_c - (f-1)q\mu_c + t\mu \tag{28}$$

which, with eqs 21−25, leads to $k_{bb} = 1$. The central bond b is adjacent to only one interarm bond, $b+1$, and the corresponding element of the matrix **K** is given by

$$k_{b+1,b} = -(f-1)qt\mu_c + t\lambda_c + \mu \tag{29}$$

It follows with eqs 21−25 that $k_{b+1,b} = 0$.

For an interarm position of the vector $\mathbf{d}_b$, the diagonal and next to diagonal elements of the column b of the matrix **K** are given by

$$k_{b-1,b} = t\lambda + \mu + t^2\mu \tag{30}$$

$$k_{bb} = \lambda + 2t\mu \tag{31}$$

and

$$k_{b+1,b} = t\lambda + t^2\mu + \mu \tag{32}$$

Using eqs 21 and 24 leads to

$$k_{bb} = 1 \tag{33}$$

and to

$$k_{b+1,b} = k_{b-1,b} = 0 \tag{34}$$

For a peripheral position of the vector $\mathbf{d}_b$ we have for the diagonal and the next to diagonal elements of **K**

$$k_{bb} = t\mu + \lambda_p \tag{35}$$

and

$$k_{b-1,b} = \mu + t\lambda_p \tag{36}$$

Together with eqs 23 and 24, we obtain that

$$k_{bb} = 1 \tag{37}$$

and that

$$k_{b-1,b} = 0 \tag{38}$$

Now let us consider the element k_{cb}, which is associated with the two nonadjacent bonds c and b connected by the shortest path ($c,x_1,\ldots,x_m,b$), where c is adjacent to x_1, x_i to x_{i+1} and x_m to b. Taking into account eq 13, we obtain

$$k_{cb} = (-q)^{\delta} t^{m-\delta} k_{x_m b} \tag{39}$$

where δ is equal to one, if the shortest path connecting the vectors $\mathbf{d}_b$ and $\mathbf{d}_c$ passes through the center of the star, and zero otherwise. Given that we have already shown that all nondiagonal elements of **K** corresponding to adjacent bonds are equal to zero, i.e. that $k_{x_m b} = 0$, we obtain that $k_{cb} = 0$ holds for all $c \neq b$.

Consequently we have proved that all diagonal elements of the matrix **K** are equal to one, whereas all off-diagonal elements are equal to zero. Therefore **K** = **1** and **VW** = **1**, as stated.

We stop to note that the case of $f = 2$ and $t = q$ leads to a linear chain with an even number of bonds. Setting $t = q$ and $f = 2$ into eqs 21 to 25 leads to $\lambda_c = \lambda$ and $\mu_c = -\mu$; i.e., it reproduces the results of a linear chain with an even number of bonds, whose vectors are oriented away from the central site.

Finally, we stop to note that the matrix **V** for star polymers already appeared in the works of Guenza and Perico,[19,20] in which, however, the matrix **W** was not obtained in analytical form.

Dendrimers. Dendrimers are macromolecules which branch repeatedly. The first generation of a dendrimer with functionality f is a star with f arms containing one bond each. The next generation is then given by attaching $(f-1)$ new bonds to each peripheral bead of the previous generation. The total number of beads of a dendrimer of generation g equals $f[(f-1)^g - 1]/(f-2) + 1$. A dendrimer of functionality $f = 3$ and generation $g = 3$ is sketched in Figure 3, where the vectors point away from the core. The numbering of the bonds occurs generationwise, as given in the figure.

To fix the ideas we focus here on dendrimers of functionality $f = 3$. Adjacent bonds are arranged tail to tail for bonds belonging to the same generation and head to tail otherwise. The elements of the matrix **V** are constructed following to eqs 11, 12, and 13, where the stiffness parameters are taken to be

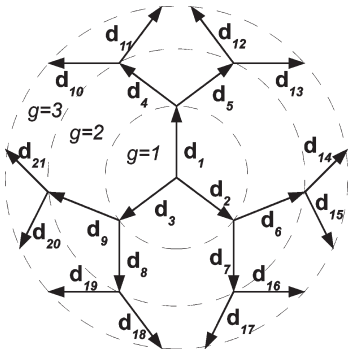

Figure 3. Bonds of a dendrimer with functionality $f = 3$ at generation $g = 3$. See the text for details.

equal, $t_i \equiv q$ for all i. For a first generation dendrimer $\mathbf{V}$ is given by

$$\mathbf{V} = \begin{pmatrix} 1 & -q & -q \\ -q & 1 & -q \\ -q & -q & 1 \end{pmatrix} \tag{40}$$

and the corresponding matrix $\mathbf{W}$ by

$$\mathbf{W} = \alpha \begin{pmatrix} -1+q & -q & -q \\ -q & -1+q & -q \\ -q & -q & -1+q \end{pmatrix} \tag{41}$$

where $\alpha = 1/(-1+q+2q^2)$.

For a second generation dendrimer, $g=2$, one has for the $\mathbf{V}$ the following structure:

$$\mathbf{V} = \begin{pmatrix} \mathbf{B}_{11} & \mathbf{B}_{12} \\ \mathbf{B}_{21} & \mathbf{B}_{22} \end{pmatrix} \tag{42}$$

where $\mathbf{B}_{11}$ is a 3×3, $\mathbf{B}_{12}$ a 3×6, $\mathbf{B}_{21} = \mathbf{B}_{12}^T$ a 6×3, and $\mathbf{B}_{22}$ a 6×6 matrix. Moreover

$$\mathbf{B}_{11} = \begin{pmatrix} 1 & -q & -q \\ -q & 1 & -q \\ -q & -q & 1 \end{pmatrix} \tag{43}$$

$$\mathbf{B}_{12} = \begin{pmatrix} q & q & -q^2 & -q^2 & -q^2 & -q^2 \\ -q^2 & -q^2 & q & q & -q^2 & -q^2 \\ -q^2 & -q^2 & -q^2 & -q^2 & q & q \end{pmatrix} \tag{44}$$

and

$$\mathbf{B}_{22} = \begin{pmatrix} 1 & -q & -q^3 & -q^3 & -q^3 & -q^3 \\ -q & 1 & -q^3 & -q^3 & -q^3 & -q^3 \\ -q^3 & -q^3 & 1 & -q & -q^3 & -q^3 \\ -q^3 & -q^3 & -q & 1 & -q^3 & -q^3 \\ -q^3 & -q^3 & -q^3 & -q^3 & 1 & -q \\ -q^3 & -q^3 & -q^3 & -q^3 & -q & 1 \end{pmatrix} \tag{45}$$

The matrix $\mathbf{W}$ corresponding to $\mathbf{V}$ has a structure similar to eq 42, namely

$$\mathbf{W} = \begin{pmatrix} \mathbf{C}_{11} & \mathbf{C}_{12} \\ \mathbf{C}_{21} & \mathbf{C}_{22} \end{pmatrix} \tag{46}$$

In eq 46

$$\mathbf{C}_{11} = \alpha \begin{pmatrix} -1+q-2q^2 & -q & -q \\ -q & -1+q-2q^2 & -q \\ -q & -q & -1+q-2q^2 \end{pmatrix} \tag{47}$$

$$\mathbf{C}_{12} = q\alpha \begin{pmatrix} 1 & 1 & 0 & 0 & 0 & 0 \\ 0 & 0 & 1 & 1 & 0 & 0 \\ 0 & 0 & 0 & 0 & 1 & 1 \end{pmatrix} \tag{48}$$

$\mathbf{C}_{21} = \mathbf{C}_{12}^T$ and

$$\mathbf{C}_{22} = \alpha \begin{pmatrix} -1+q & -q & 0 & 0 & 0 & 0 \\ -q & -1+q & 0 & 0 & 0 & 0 \\ 0 & 0 & -1+q & -q & 0 & 0 \\ 0 & 0 & -q & -1+q & 0 & 0 \\ 0 & 0 & 0 & 0 & -1+q & -q \\ 0 & 0 & 0 & 0 & -q & -1+q \end{pmatrix} \tag{49}$$

The parameter α in eqs 47−49 equals $\alpha = 1/(-1+q+2q^2)$.

For any arbitrary generation, e.g., g, the matrix $\mathbf{V} = (V_{ab})$ has the following structure: The diagonal elements are always unity. The elements associated with adjacent bonds $\mathbf{d}_a$ and $\mathbf{d}_b$ are equal to $\pm q$, where the sign is minus when the vectors $\mathbf{d}_a$ and $\mathbf{d}_b$ belong to the same generation and plus if they are from different generations. For nonadjacent bonds, e.g., $\mathbf{d}_x$ and $\mathbf{d}_y$, the elements $V_{xy} = V_{yx}$ equal $\pm q^{n+1}$, where n is the number of vectors $(\mathbf{d}_{z_1},\ldots,\mathbf{d}_{z_n})$ in the shortest path $(x, z_1,\ldots,z_n,y)$ which connects the vectors $\mathbf{d}_x$ and $\mathbf{d}_y$. The sign is plus when all the vectors $(\mathbf{d}_x,\mathbf{d}_{z_1},\ldots,\mathbf{d}_{z_n},\mathbf{d}_y)$ belong to different generations and is minus in all other cases.

The elements of the matrix $\mathbf{W}$ for generation g (as in the case $g=2$ given in eqs 46−49) take only five different values. The diagonal elements of the nonperipheral bonds (at generation 1 to $(g-1)$) are equal to $(-1+q-2q^2)/(-1+q+2q^2) \equiv \nu$, and those of the peripheral bonds (at generation g) are equal to $(-1+q)/(-1+q+2q^2) \equiv \nu_p$. If the bonds $\mathbf{d}_a$ an $\mathbf{d}_b$ are adjacent, then the corresponding elements $W_{ab} = W_{ba}$ equal $\pm q/(-1+q+2q^2) \equiv \pm\xi$, where the plus sign holds for segments belonging to different generations and the minus sign otherwise. The elements corresponding to nonadjacent bonds are always equal to zero.

The proof that $\mathbf{VW} = \mathbf{1}$ is as follows. We start by setting $\mathbf{K} = \mathbf{VW}$ and show that $\mathbf{K} = \mathbf{1}$. The proof depends on whether $\mathbf{d}_b$ is in a nonperipheral, Figure 4a or Figure 4b, or in a peripheral position, Figure 4c. A nonperipheral $\mathbf{d}_b$ has four nearest neighbors $\mathbf{d}_a$, $\mathbf{d}_d$, $\mathbf{d}_c$, and $\mathbf{d}_e$, whereas a peripheral $\mathbf{d}_b$ has only

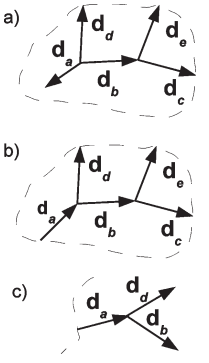

Figure 4. Domains from a dendrimer molecule. In parts a and b, the vector $\mathbf{d}_b$ is in an internal and in part c in a peripheral position. In part a, the vectors $\mathbf{d}_a$, $\mathbf{d}_b$ and $\mathbf{d}_d$ belong to the same and in part b to different generations.

two neighbors $\mathbf{d}_a$ and $\mathbf{d}_e$. In both cases, we treat first, columnwise, the diagonal elements of **K** and the elements of **K** associated with adjacent bonds. Then we focus on the elements of **K** related to nonadjacent bonds.

We begin with $\mathbf{d}_b$ being nonperipheral; see parts a and b of Figure 4. The diagonal element of the matrix **K** is given by

$$k_{bb} = \nu + 4q\xi \tag{50}$$

However, the nondiagonal elements corresponding to the adjacent nearest neighbors are for Figure 4a

$$-k_{ab} = -k_{db} = k_{cb} = k_{eb} = \xi - q\xi + q\nu + 2q^2\xi \tag{51}$$

and for Figure 4b

$$+k_{ab} = -k_{db} = k_{cb} = k_{eb} = \xi - q\xi + q\nu + 2q^2\xi \tag{52}$$

Here we have used the constants ν and ξ introduced above. When we substitute their expressions as a function of q into eqs 50−52, we obtain $k_{bb} = 1$ and $k_{ab} = k_{db} = k_{cb} = k_{eb} = 0$.

When $\mathbf{d}_b$ is peripheral, Figure 4c, we have as diagonal element

$$k_{bb} = \nu_p + 2q\xi \tag{53}$$

and for the nondiagonal elements corresponding to the adjacent nearest neighbors:

$$k_{ab} = -k_{db} = \xi - q\xi + q\nu_p \tag{54}$$

After substitution of ν_p and ξ we obtain that $k_{bb} = 1$ and $k_{ab} = k_{db} = 0$.

Finally, as before, for the elements of **K** corresponding to any two nonadjacent bonds, e.g., x and y, connected by a shortest path ($x, z_1, \ldots, z_m, y$), eq 13 yields, depending on the bonds' orientation

$$k_{xy} = q^m k_{z_m b} \tag{55}$$

or

$$k_{xy} = -q^m k_{z_m b} \tag{56}$$

Given that $k_{z_m b} = 0$ it follows that $k_{xy} = 0$.

Thus the diagonal elements of **K** are all unity, whereas all nondiagonal elements vanish. It follows that $\mathbf{K} = \mathbf{1}$, as previously claimed.

Dynamics

We now make use of the generalization of the Rouse-model to describe the dynamics of semiflexible structures obtained by replacing (in the spirit of ref 15) the potential V_R, eq 8, through the potential V_{BZ}, eq 9. By this the Langevin equation of the Rouse-model, eq 6 turns into

$$\zeta \frac{\partial \mathbf{R}_\alpha(t)}{\partial t} + K\mathbf{A}^{BZ}\mathbf{R}_\alpha(t) = \mathbf{F}_\alpha(t) \tag{57}$$

where now, according eqs 3 and 9, $\mathbf{A}^{BZ}$ is given through

$$\mathbf{A}^{BZ} = \mathbf{GWG}^T \tag{58}$$

The important feature which we now find (*vide infra*) is that the expressions for the dielectric relaxation change with respect to what holds for the simple Rouse model. On the other hand, following the classical derivation,[33] the expressions for the mechanical moduli stay unaffected by the change from $\mathbf{A}^R$ to $\mathbf{A}^{BZ}$, the only change consisting in different values for the eigenvalues.

Equation 57 can be solved using the normal mode transformation

$$r_{\alpha i}(t) = \sum_k C_{ik} Q_{\alpha k}(t) \tag{59}$$

where $\mathbf{C} = \{C_{ik}\}$ is the matrix which diagonalizes the matrix $\mathbf{A}^{BZ}$

$$\mathbf{C}^{-1}\mathbf{GWG}^T\mathbf{C} = \mathbf{\Lambda} \tag{60}$$

Here it should be noted that the matrix **C** depends on the stiffness parameters $\{t_i\}$. In the limit $\{t_i \to 0\}$ we have $\mathbf{W} = \mathbf{1}$; therefore the matrix $\mathbf{C}(\{t_i = 0\})$ will diagonalize the matrix $\mathbf{GG}^T$, i.e., the Rouse connectivity matrix $\mathbf{A}^R$. Under the transformation given by eq 59 the Langevin equation simplifies to

$$\zeta \frac{\partial}{\partial t} Q_{\alpha k}(t) + K\lambda_k Q_{\alpha k}(t) = \hat{f}_{\alpha k}(t) \tag{61}$$

where $\hat{f}_{\alpha k}(t) = \sum_i (\mathbf{C}^{-1})_{ki} f_{\alpha k}(t)$. Hence $\langle \hat{f}_{\alpha k}(t)\hat{f}_{\beta m}(t')\rangle = 2k_B T\zeta\delta_{km}\delta_{\alpha\beta}\delta(t - t')$ and $\langle \hat{\mathbf{f}}_k(t)\rangle = 0$, so that, from eq 61 the following relations hold:[33,34]

$$\langle (Q_{\alpha 1}(t) - Q_{\alpha 1}(0))(Q_{\beta 1}(t) - Q_{\beta 1}(0))\rangle = \delta_{\alpha\beta}\frac{2k_B T}{N\zeta}t \tag{62}$$

and

$$\langle Q_{\alpha k}(t) Q_{\beta m}(0)\rangle = \delta_{\alpha\beta}\delta_{km}\langle Q_{\beta m}{}^2\rangle e^{-t/\tau_m} \quad (k, m = 2, \ldots, N) \tag{63}$$

where $Q_{\beta m}{}^2 = k_B T/(K\lambda_m)$ and $\tau_m = \zeta/(K\lambda_m) = \tau_0/\lambda_m$. Here the $\{\lambda_m\}$ are the eigenvalues which build the diagonal matrix $\mathbf{\Lambda}$. For a connected network the $N \times N$ matrix $\mathbf{A}^{BZ}$ has rank $(N - 1)$. This is due to the fact that both **W** and **G** have rank $(N - 1)$: **W** because it is a $(N - 1) \times (N - 1)$ matrix and has an inverse; **G** because it is the incidence matrix of a connected network of N sites.[27] Therefore the matrix $\mathbf{A}^{BZ}$ has exactly one nondegenerate eigenvalue, $\lambda_1 = 0$.[7] The knowledge of the nonzero eigenvalues $\{\lambda_m\}$ and of the eigenvectors of $\mathbf{A}^{BZ}$ is sufficient for determining many of the dynamical properties of GGS, such as the mechanical and dielectric relaxation.

We now follow the changes in the relaxation forms due to the inclusion of stiffness according to eqs 57 and 58 and start with the dielectric features. Dielectric relaxation is related to the frequency-dependent complex dielectric susceptibility, $\varepsilon^*(\omega)$. One usually focuses on $\Delta\varepsilon^*(\omega)$, which is introduced as follows:

$$\Delta\varepsilon^*(\omega) = \frac{\varepsilon^*(\omega) - \varepsilon_\infty}{\varepsilon_0 - \varepsilon_\infty} \tag{64}$$

In eq 64, ε_0 and ε_∞ denote the limiting low- and high-frequency dielectric constants, respectively. In general, for the $\Delta\varepsilon^*(\omega)$ of polar molecules embedded in nonpolar solvents under an oscillatory electric field $E = E_0\exp(i\omega t)$, one has[35]

$$\Delta\varepsilon^*(\omega) \simeq \int_0^\infty \left(-\frac{d}{dt}C_0(\mathbf{M}; t)\right)\exp(-i\omega t)\, dt \tag{65}$$

when the local fields are not important. In eq 65, $C_0(\mathbf{M};t)$ is the normalized autocorrelation function of the total dipole moment $\mathbf{M}(t)$ of the polymer system:

$$C_0(\mathbf{M}; t) = \frac{\langle \mathbf{M}(0)\mathbf{M}(t)\rangle}{\langle \mathbf{M}^2(0)\rangle} \tag{66}$$

In general, the expression for $\Delta\varepsilon^*(\omega)$, eq 65, cannot be reduced to a simple, compact form. However, we proceed to show that this becomes possible under certain conditions.

Here we focus on the dielectric response of a polar GGS whose bonds possess dipole moments directed along them, the type A-model according Stockmayer's classification.[26] In this model one assigns a longitudinal dipole moment $\mathbf{m}_a$ to each bond $\mathbf{d}_a$ of the GGS, so that $|\mathbf{m}_a|$ is proportional to $|\mathbf{d}_a|$. On the other hand, $\mathbf{m}_a$ can be oriented parallel or antiparallel to $\mathbf{d}_a$. The total dipole moment $\mathbf{M}(t)$ of the GGS is then given by:

$$\mathbf{M}(t) = \sum_{a=1}^{N-1} \mu_a \mathbf{d}_a(t) \tag{67}$$

where $\mu_a = \mu e_a$ is the dipole moment per unit length, and $e_a \in \{+1, -1\}$ gives the orientation.

To proceed, we assume that the orientations $\{e_a\}$ are random and uncorrelated.[36,37] This key feature simplifies the situation considerably. Denoting the average over the distinct dipole moments orientations by $\langle \ldots \rangle_{or}$ we obtain for the autocorrelation function of $\mathbf{M}(t)$:

$$\begin{aligned}\langle \mathbf{M}(0)\mathbf{M}(t)\rangle &= \mu^2 \sum_{a,b} \langle e_a e_b\rangle_{or} \langle \mathbf{d}_a(0)\mathbf{d}_b(t)\rangle \\ &= \mu^2 \sum_{a} \langle \mathbf{d}_a(0)\mathbf{d}_a(t)\rangle \end{aligned} \tag{68}$$

In deriving eq 68 we made use of the condition of random orientation, $\langle e_a e_b\rangle_{or} = \delta_{ab}$. Using the definition of the incidence matrix $\mathbf{G}$, eq 3, and the normal mode transformation, eq 59, we obtain

$$\begin{aligned}\langle \mathbf{M}(0)\mathbf{M}(t)\rangle &= \mu^2 \sum_{a,i,j,k,l} \langle ((\mathbf{G}^T)_{ai} C_{ik}) \mathbf{Q}_k(0) \cdot ((\mathbf{G}^T)_{aj} C_{jl}) \mathbf{Q}_l(t)\rangle \\ &= \mu^2 \sum_{k=2}^{N} \langle \mathbf{Q}_k^2\rangle (\mathbf{C}^T \mathbf{G}\mathbf{G}^T \mathbf{C})_{kk} \exp(-t/\tau_k) \\ &\quad + \mu^2 \langle \mathbf{Q}_1(0)\mathbf{Q}_1(t)\rangle (\mathbf{C}^T \mathbf{G}\mathbf{G}^T \mathbf{C})_{11} \end{aligned} \tag{69}$$

where $\langle \mathbf{Q}_k^2\rangle = 3k_BT/(K\lambda_k)$. Note that the first column of $\mathbf{C}$, which corresponds to the eigenvalue $\lambda_1 = 0$, is given by the vector $(1,\ldots,1)^T/N^{1/2}$. This vector is also an eigenvector of $\mathbf{G}\mathbf{G}^T = \mathbf{A}^R$, because of the particular structure of the incidence matrix $\mathbf{G}$: In each row it has only one entry -1 and only one entry $+1$. Therefore $(\mathbf{C}^T\mathbf{G}\mathbf{G}^T\mathbf{C})_{11} = 0$. Then one has for the normalized autocorrelation function of the dipole moment:

$$C_0(\mathbf{M}; t) = \frac{\Sigma_k \gamma_k \exp(-t\lambda_k/\tau_0)}{\Sigma_k \gamma_k} \tag{70}$$

where we introduced the notation $\gamma_k \equiv (\mathbf{C}^T\mathbf{G}\mathbf{G}^T\mathbf{C})_{kk}/\lambda_k$. After substitution of the last equation into eq 65, the real and imaginary parts of the complex susceptibility $\Delta\varepsilon^*(\omega) = \Delta\varepsilon'(\omega) - i\Delta\varepsilon''(\omega)$ follow

$$\Delta\varepsilon'(\omega) = \frac{1}{\sum_{k=2}^{N} \gamma_k} \sum_{k=2}^{N} \frac{\gamma_k}{(1 + (\omega\tau_0/\lambda_k)^2)} \tag{71}$$

and

$$\Delta\varepsilon''(\omega) = \frac{1}{\sum_{k=2}^{N} \gamma_k} \sum_{k=2}^{N} \frac{\gamma_k \omega\tau_0/\lambda_k}{(1 + (\omega\tau_0/\lambda_k)^2)} \tag{72}$$

One should note the change from the case of usual Rouse model: in the case of semiflexible structures one has to know not only the eigenvalues $\{\lambda_k\}$, but also the $\{\gamma_k\}$. In the flexible limit all $\{\gamma_k\}$ equal unity, and we recover the usual formulas for the Rouse model.[36,37]

Another useful experimental method for investigating the dynamics is the mechanical relaxation.[33] Here we follow closely the derivation of ref 34, and we obtain (distinct from the dielectric relaxation) the same functional forms for $\mathbf{A}^R$ and for $\mathbf{A}^{BZ}$. To determine the mechanical moduli one subjects the sample to a harmonic strain, e.g., $\mathbf{s}(t) = \mathbf{s}_0 \cos(\omega t)$, which leads to the appearance of a velocity term in the Langevin equation, which equals $\mathbf{s}(t)\mathbf{r}_i$ under the assumption that all the $\{\mathbf{r}_i\}$ are uncoupled. Focusing only on one component of the strain, e.g., $s_{\alpha\beta}(t) \equiv s(t)$, we obtain

$$\zeta \frac{\partial}{\partial t} r_{\alpha i}(t) + \frac{\partial}{\partial r_{\alpha i}} V_{BZ}(\{\mathbf{r}_k\}) = f_{\alpha i}(t) + s(t) r_{\beta i}(t) \tag{73}$$

In the rigid limit, we have a strong coupling between the position variables. Therefore eq 73 can hold only in the semiflexible regime, very far from the rigid limit. Now the response to a harmonic strain field is a stress

$$\sigma_{\alpha\beta} = -(\nu/N) \sum_{n} \langle F_{\alpha n} r_{\beta n}\rangle \tag{74}$$

where the multiplier $\nu = (N/V)$ is the number of monomers per unit volume and the force $F_{\alpha n}$ is due to the potential $V_{BZ}(\{\mathbf{r}_i\})$, being given by

$$F_{\alpha n} = -\frac{\partial}{\partial r_{\alpha n}} V_{BZ}(\{\mathbf{r}_i\}) \tag{75}$$

Using the normal mode transformation, eq 59, the Langevin equation, eq 73, simplifies to

$$\zeta \frac{\partial}{\partial t} Q_{\alpha k}(t) + K\lambda_k Q_{\alpha k}(t) = \hat{f}_{\alpha k}(t) + s(t) Q_{\beta k}(t) \tag{76}$$

where we have the same notations as in eq 61. The $\alpha\beta$-component of the stress tensor reads as follows:

$$\sigma_{\alpha\beta} = (K\nu/N) \sum_{k} \lambda_k \langle Q_{\alpha k}(t) Q_{\beta k}(t)\rangle \tag{77}$$

The correlation function $\langle Q_{\alpha k}(t) Q_{\beta k}(t)\rangle$ follows from eq 76:

$$\langle Q_{\alpha k}(t) Q_{\beta k}(t)\rangle = \frac{k_BT}{K\lambda_k} \int_{-\infty}^{t} dt' \exp[-2(t-t')/\tau_p] s(t') \tag{78}$$

Substituting eq 78 into eq 77 gives

$$\sigma_{\alpha\beta} = \int_{-\infty}^{t} dt' \, G(t-t') s(t') \tag{79}$$

where $G(t)$ reads

$$G(t) = (\nu k_BT/N) \sum_{k} \exp(-2t/\tau_k) \tag{80}$$

by which we recover the classical expression, eq 5.84 of ref 34. Thus, in the usual way, the complex shear modulus $G^*(\omega)$, has as real, $G'(\omega)$, and imaginary, $G''(\omega)$, components

$$G'(\omega) = \frac{\nu k_BT}{N} \sum_{k=2}^{N} \frac{(\omega\tau_0/2\lambda_k)^2}{1 + (\omega\tau_0/2\lambda_k)^2} \tag{81}$$

and

$$G''(\omega) = \frac{\nu k_B T}{N} \sum_{k=2}^{N} \frac{\omega\tau_0/2\lambda_k}{1 + (\omega\tau_0/2\lambda_k)^2} \tag{82}$$

where, as below eq 63, we set $\tau_0 = \zeta/K$. Here it is practical to introduce the reduced variables denoted by $[G'(\omega)]$ and $[G''(\omega)]$ and defined through[3]

$$[G'(\omega)] = \frac{1}{N} \sum_{k=2}^{N} \frac{(\omega\tau_0/2\lambda_k)^2}{1 + (\omega\tau_0/2\lambda_k)^2} \tag{83}$$

and

$$[G''(\omega)] = \frac{1}{N} \sum_{k=2}^{N} \frac{\omega\tau_0/2\lambda_k}{1 + (\omega\tau_0/2\lambda_k)^2} \tag{84}$$

We conclude that in terms of the BZ-model the moduli of semiflexible polymers depend (as in the pure Rouse case) only on the eigenvalues $\{\lambda_k\}$. This differs from the situation for the dielectric relaxation, where also the knowledge of the eigenvectors is required. The only exception to this is the pure Rouse-model, where for $N \gg 1$ the following expressions hold exactly:[3]

$$\Delta\varepsilon'(\omega) = 1 - [G'(2\omega)] \tag{85}$$

and

$$\Delta\varepsilon''(\omega) = [G''(2\omega)] \tag{86}$$

Results and Discussion

Based on the results obtained in the previous chapters, we evaluate now for semiflexible polymers the dynamical functions we are interested in, namely the moduli $G'(\omega)$ and $G''(\omega)$ as well as the dielectric forms $\Delta\varepsilon'(\omega)$ and $\Delta\varepsilon''(\omega)$. We recall the universal scaling relations which hold for all finite networks: for very small ω one has $G'(\omega) \sim \omega^2$, $G''(\omega) \sim \omega$, $\Delta\varepsilon'(\omega) \sim \omega^0$ and $\Delta\varepsilon''(\omega) \sim \omega$; for very large ω one has $G'(\omega) \sim \omega^0$, $G''(\omega) \sim \omega^{-1}$, $\Delta\varepsilon'(\omega) \sim \omega^{-2}$ and $\Delta\varepsilon''(\omega) \sim \omega^{-1}$. As in all related cases, the particular structure of the network can be seen only in the in-between region. For the mechanical relaxation the dimensionless units $\nu k_B T = 1$ are chosen, so that $G'(\omega) = [G'(\omega)]$ and $G''(\omega) = [G''(\omega)]$.

We start by considering a six-arm star with $n = 15$ segments per arm and vary the stiffness parameter t, while at the same time assuming that q, the stiffness parameter for the bonds stemming from the center bead equals $q = t/5$. We now plot in Figure 5 the mechanical storage $G'(\omega)$ and loss $G''(\omega)$ moduli and in Figure 6 the real and imaginary parts, $\Delta\varepsilon'(\omega)$ and $\Delta\varepsilon''(\omega)$, of the dielectric susceptibility. The range of parameters extends from the Rouse-case, $t = 0$, up to $t = 0.7$.

Focusing first on Figure 5, we see for the Rouse-case, in the absence of any stiffness, a global behavior very reminiscent of linear chains, where the curves in the intermediate domain scale—both for $G'(\omega)$ and for $G''(\omega)$—with the power $^1/_2$. The fact that we have a star and not individual chains is evidenced in the low-ω range by the appearance of a small bump superimposed on the smooth underlying curve in the transition region form the long time (small ω) to the intermediate domain. With increasing stiffness the picture changes, however. For larger t, the dynamical intermediate range becomes wider and thus the curves get broader. Furthermore, one witnesses the appearance of low lying modes, whose global influence is to change the apparent slope in the intermediate regime. In Figure 5, we have indicated this

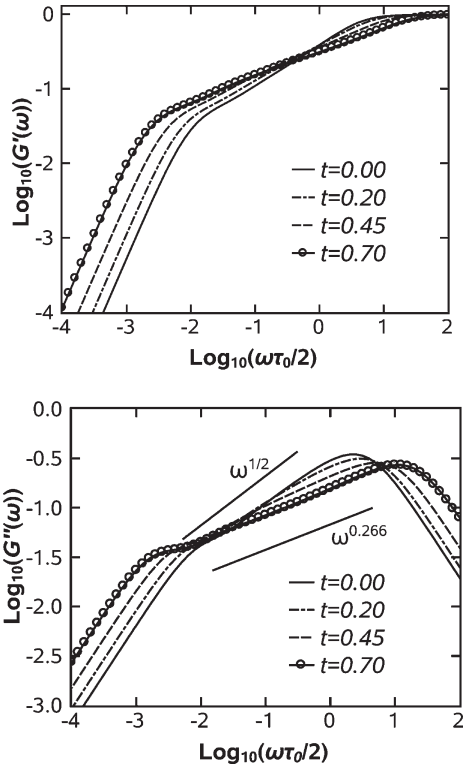

Figure 5. Storage $G'(\omega)$ and loss $G''(\omega)$ moduli for a star with $f = 6$ arms and $n = 15$ segments in each arm, plotted for different degrees of stiffness t. Here the stiffness of the core is always given by $q = t/(f-1)$.

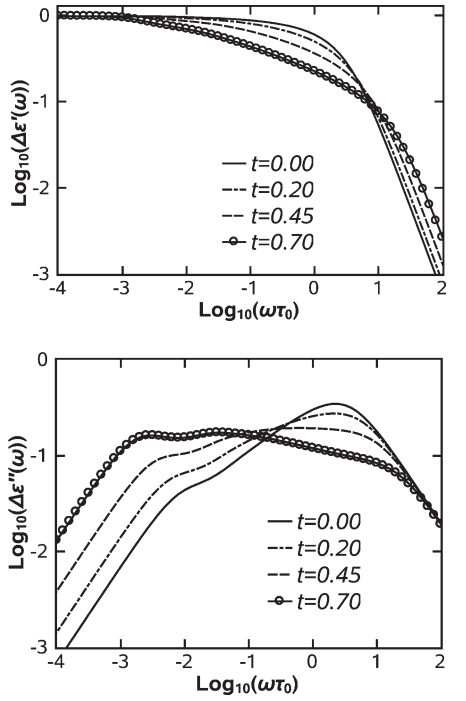

Figure 6. Real $\Delta\varepsilon'(\omega)$ and imaginary $\Delta\varepsilon''(\omega)$ parts of the complex susceptibility for a star with $f = 6$ arms and $n = 15$ segments in each arm. The parameters are as in Figure 5.

change in slope from being close to $^1/_2$ for $t = 0$ to being close to $^1/_4$ for $t = 0.7$; the best fit to the $G''(\omega)$ curve for $t = 0.7$ gives an exponent of 0.266. Now a $^1/_4$ exponent is the hallmark of semiflexible chains, see refs 38 and 39

Even more impressive are the findings for $\Delta\varepsilon'(\omega)$ and for $\Delta\varepsilon''(\omega)$, presented in Figure 6. As mentioned before, in the

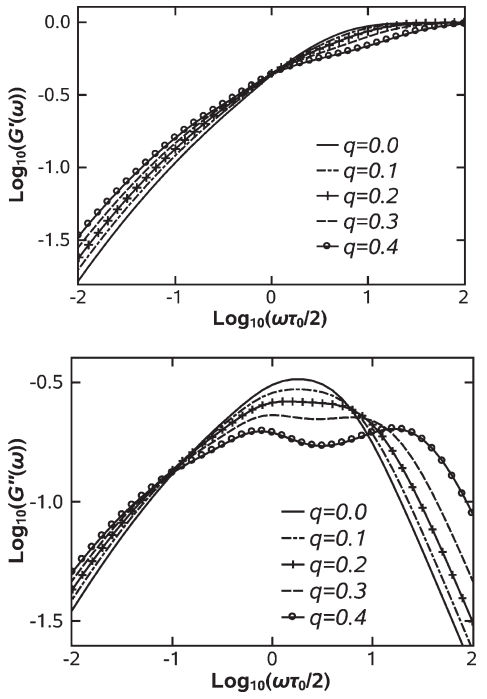

Figure 7. Storage $G'(\omega)$ and loss $G''(\omega)$ moduli for a dendrimer of generation $g = 8$ and functionality $f = 3$ plotted for different degrees of stiffness q.

presence of stiffness the simple relations[3] between $G'(\omega)$ and $\Delta\varepsilon'(\omega)$ on the one hand and $G''(\omega)$ and $\Delta\varepsilon''(\omega)$ on the other, eqs 85 and 86, do not hold exactly anymore. While with increasing t the curve $\Delta\varepsilon'(\omega)$ stays quite smooth and manifests mainly the widening of the dynamical range, in $\Delta\varepsilon''(\omega)$ the additional low-lying modes that appear at the expense of the high lying ones become clearly evident. In our theoretical framework, we are thus led for t large to a quite rich structure.

We now turn to the case of dendrimers and consider a structure with functionality $f = 3$ at the generation $g = 8$. The forms of the mechanical and of the dielectric relaxation are given in Figure 7 and Figure 8, respectively. Here we encounter only the functionalities $f = 3$ for the internal and $f = 1$ for the peripheral sites. Thus here the semiflexibility depends only on the parameter q, see, e.g., eq 40. In Figure 7 and Figure 8, we vary q from the pure Rouse-case, $q = 0$, to the semiflexible case $q = 0.4$. As for star polymers, here again we find an increase in the intensity of the low lying modes at the expense of the high lying ones. The Rouse behavior in Figure 7 is typical for dendrimers; for these no scaling is observable in the intermediate range, the $G'(\omega)$ and $G''(\omega)$ curves being best described by logarithmic expressions.[3,40] Introducing stiffness lets the $G'(\omega)$ curve increase more slowly, see Figure 7. Even more pronounced is the effect of stiffness on $G''(\omega)$: Here, with increasing stiffness, the curves develop a minimum in the intermediate range, fact also observed in previous works.[7,21]

The dielectric relaxation forms, $\Delta\varepsilon'(\omega)$ and $\Delta\varepsilon''(\omega)$, present similar features. First, in the Rouse case, $G''(\omega)$ and $\Delta\varepsilon''(\omega)$ behave in the same way, see eq 86, an aspect which gets lost with increasing q. Introducing stiffness leads to changes in the forms of $G''(\omega)$ and of $\Delta\varepsilon''(\omega)$. Thus, whereas in the high-ω regime the $G''(\omega)$ curves shift to higher frequencies, the $\Delta\varepsilon''(\omega)$ curves have the tendency to lay strictly below the $q = 0$ curve. The low-ω regime is different: Here the increase in $\Delta\varepsilon''(\omega)$ is more accentuated than in $G''(\omega)$. In fact Figure 8 displays for $\Delta\varepsilon''(\omega)$ a large shift in its maximum toward lower ω values. So that the widening of $\Delta\varepsilon''(\omega)$ occurs in the direction of the slow modes, whereas $G''(\omega)$ widens in both directions.

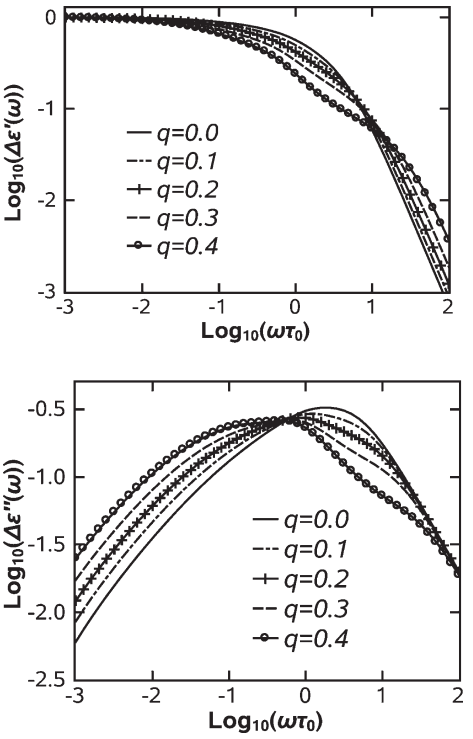

Figure 8. Real $\Delta\varepsilon'(\omega)$ and imaginary $\Delta\varepsilon''(\omega)$ parts of the complex susceptibility for a dendrimer of generation $g = 8$ and functionality $f = 3$ plotted for different degrees of stiffness q.

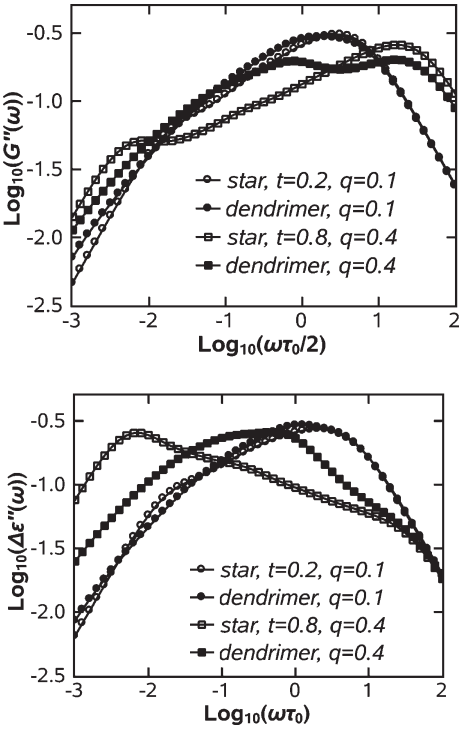

Figure 9. Loss modulus $G''(\omega)$ and the imaginary part $\Delta\varepsilon''(\omega)$ of the complex susceptibility plotted for a dendrimer of generation $g = 8$ and functionality $f = 3$ and for a three-arm-star with $n = 8$ segments per arm. The degrees of stiffness q and t are as indicated.

Given the profound differences in the relaxation behaviors of star polymers and of dendrimers, we present in Figure 9 a direct comparison between two such structures. For this, we allow in both cases the maximal chemical distance from the central monomer (the core) to the peripheral monomers to be the same,

namely 8. Furthermore, we fix for both objects the functionality to the value $f = 3$. This allows us (in the absence of excluded volume effects) to have for both molecules the same averaged core−periphery distance, at the cost of having different numbers of monomers in each molecule, namely $N = 766$ in the dendrimer and $N = 25$ in the star polymer. In Figure 9 we display for both molecules $G''(\omega)$ and $\Delta\varepsilon''(\omega)$ under two district stiffness conditions: In the first case we take a quite low degree of stiffness, by using $q = 0.1$ and $t = 0.2$, in the second case a quite high degree of stiffness, by assuming $q = 0.4$ and $t = 0.8$. While in the first case the relaxation patterns are not very different from the fully flexible Rouse-behavior, Figure 9 renders clear the considerable changes that occur by going to high degrees of stiffness; in the figure the extension of the intermediate regime and the fact that for $\Delta\varepsilon''(\omega)$ the widening happens only on the low frequency side are clearly visible. Moreover, Figure 9 shows with increasing stiffness more drastic changes in $\Delta\varepsilon''(\omega)$ than in $G''(\omega)$.

Some of our theoretical results are also reflected in recent experiments on branched polymers, albeit in melts, such as on Cayley-tree-type polyisoprene (CT-PI).[41] The corresponding mechanical and dielectric relaxation data found in the experiments by Watanabe et al. show in the intermediate frequency region that $G''(\omega)$ scales approximately as $\omega^{1/4}$, see Figure 2 of ref 41, a result typical for semiflexible spacers. This finding is also in agreement with recent simulations on melts of semiflexible chains.[39,42] In the measurements by Watanabe et al. the imaginary part of the dielectric relaxation, $\Delta\varepsilon''(\omega)$, displays a plateau-like behavior, see Figure 3 of ref 41, a result similar to our Figure 6. Furthermore, recent rheological experiments on dendrimers[43] show for $G''(\omega)$ a local minimum in the region of intermediate frequencies, as we also find in Figure 7.

We close by noting that extensions of the BZ-model for melts made out of *semiflexible chains* were quite successful: ref 17 reports quantitative agreement between neutron spin echo experiments and such models. Another extension of the BZ-model allowed good predictions of the NMR relaxation data and of the Debye−Waller factors for the local dynamics of proteins.[18] Based on these findings, we expect that our treatment of *semiflexible tree-like networks* in the BZ-framework will also lead to fruitful extensions and applications.

Conclusions

In this article we have studied the dynamics of semiflexible chains, stars and dendrimers. Semiflexibility is introduced by inserting geometrical restrictions on the bonds' orientations, which fact affects the shape of the potential, transforming it in the bonds' description to a nondiagonal bilinear form. Under physically reasonable assumptions leading to the matrix $\mathbf{V}$, defined by eqs 11, 12, and 13, it turns out that the matrix $\mathbf{W}$, its inverse ($\mathbf{W} = \mathbf{V}^{-1}$), is a particularly simple, sparse matrix. Thus the only nonzero off-diagonal elements of $\mathbf{W}$ correspond to adjacent bonds and the diagonal elements of $\mathbf{W}$ (corresponding to individual bonds) depend on the functionalities and stiffness parameters of the sites connected by the bond in question.

Based on the simple structure of the matrices $\mathbf{W}$, we have investigated both the mechanical and the dielectric relaxation forms for dendrimers and for star polymers. It turns out that for semiflexible polymers the dielectric relaxation depends not only on the eigenvalues (as in the case for flexible polymers), but also on the eigenvectors of $\mathbf{A}^{BZ}$. This fact leads in the semiflexible case to differences between $G''(\omega)$ and $\Delta\varepsilon''(\omega)$, the latter displaying a very rich structure.

Acknowledgment. The authors acknowledge the support of the Deutsche Forschungsgemeinschaft and of the Fonds der Chemischen Industrie.

References and Notes

(1) Rouse, P. E. *J. Chem. Phys.* **1953**, *21*, 1272.
(2) Zimm, B. H. *J. Chem. Phys.* **1956**, *24*, 269.
(3) Gurtovenko, A. A.; Blumen, A. *Adv. Polym. Sci.* **2005**, *182*, 171.
(4) Blumen, A.; Jurjiu, A. *J. Chem. Phys.* **2002**, *116*, 2636.
(5) Cai, C.; Chen, Z. Y. *Macromolecules* **1997**, *30*, 5104.
(6) Chen, Z. Y.; Cai, C. *Macromolecules* **1999**, *32*, 5423.
(7) von Ferber, C.; Blumen, A. *J. Chem. Phys.* **2002**, *116*, 8616.
(8) Gurtovenko, A. A.; Gotlib, Yu. Ya.; Blumen, A. *Macromolecules* **2002**, *35*, 7481.
(9) Blumen, A.; Jurjiu, A.; Koslowski, Th.; von Ferber, Ch. *Phys. Rev. E* **2003**, *67*, 061103.
(10) Blumen, A.; von Ferber, Ch.; Jurjiu, A.; Koslowski, Th. *Macromolecules* **2004**, *37*, 638.
(11) Jurjiu, A.; Koslowski, Th.; Blumen, A. *J. Chem. Phys.* **2003**, *118*, 2398.
(12) Satmarel, C.; von Ferber, C.; Blumen, A. *J. Chem. Phys.* **2005**, *123*, 034907.
(13) Galiceanu, M.; Blumen, A. *J. Chem. Phys.* **2007**, *127*, 134904.
(14) Press, W. H.; Teukolski, S. A.; Vetterling, W. T.; Flannery, B. P. *Numerical Recipes in Fortran 77*, 2nd ed.; Cambridge University Press: New York, 2003.
(15) Bixon, M.; Zwanzig, R. *J. Chem. Phys.* **1978**, *68*, 1896.
(16) Guenza, M. G. *J. Phys.: Condens. Matter* **2008**, *20*, 1.
(17) Zamponi, M.; Wischnewski, A.; Monkenbusch, M.; Willner, L.; Richter, D.; Falus, P.; Farago, B.; Guenza, M. G. *J. Phys. Chem. B* **2008**, *112*, 16220.
(18) Caballero-Manrique, E.; Bray, J. K.; Deutschman, W. A.; Dahlquist, F. W.; Guenza, M. G. *Biophys. J.* **2007**, *93*, 4128.
(19) Guenza, M.; Mormino, M.; Perico, A. *Macromolecules* **1991**, *24*, 6168.
(20) Guenza, M.; Perico, A. *Macromolecules* **1992**, *25*, 5942.
(21) La Ferla, R. *J. Chem. Phys.* **1997**, *106*, 688.
(22) Kratky, O.; Porod, G. *Recl. Trav. Chim. Pays-Bas* **1949**, *68*, 1106.
(23) Bawendi, M. G.; Freed, K. F. *J. Chem. Phys.* **1985**, *83*, 2491.
(24) Lagowski, J. B.; Noolandi, J.; Nickel, B. *J. Chem. Phys.* **1991**, *95*, 1266.
(25) Harnau, L.; Winkler, R. G.; Reineker, P. *J. Chem. Phys.* **1995**, *102*, 7750.
(26) Stockmayer, W. H. *Pure Appl. Chem.* **1967**, *15*, 539.
(27) Biggs, N. *Algebraic Graph Theory*, 2nd ed.; Cambridge University Press: Cambridge, U.K., 1993.
(28) Zwanzig, R. *J. Chem. Phys.* **1974**, *60*, 2717.
(29) Mansfield, M. L.; Stockmayer, W. H. *Macromolecules* **1980**, *13*, 1713.
(30) Guenza, M.; Perico, A. *J. Chem. Phys.* **1986**, *84*, 510.
(31) Guenza, M.; Perico, A. *J. Chem. Phys.* **1985**, *83*, 3103.
(32) Winkler, R. G.; Reineker, P.; Harnau, L. *J. Chem. Phys.* **1994**, *101*, 8119.
(33) Doi, M.; Edwards, S. F. *The Theory of Polymer Dynamics*; Clarendon Press: Oxford, U.K., 1986.
(34) Doi, M. *Introduction to Polymer Physics*; Clarendon Press: Oxford, U.K., 1996.
(35) Glarum, S. H. *J. Chem. Phys.* **1959**, *33*, 1371.
(36) Gotlib, Yu. Ya.; Gurtovenko, A. A. *Macromol. Theory Simul.* **1996**, *5*, 969.
(37) Gurtovenko, A. A.; Blumen, A. *Macromolecules* **2002**, *35*, 3288.
(38) Hearst, J. E.; Harris, R. A.; Beals, E. *J. Chem. Phys.* **1966**, *45*, 3106.
(39) Bulacu, M.; van der Giessen, E. *J. Chem. Phys.* **2005**, *123*, 114901.
(40) Biswas, P.; Kant, R.; Blumen, A. *J. Chem. Phys.* **2001**, *114*, 2430.
(41) Watanabe, H.; Matsumiya, Y.; van Ruymbeke, E.; Vlassopoulos, D.; Hadjichristidis, N. *Macromolecules* **2008**, *41*, 6110.
(42) Steinhauser, M. O.; Schneider, J.; Blumen, A. *J. Chem. Phys.* **2009**, *130*, 164902.
(43) Lee, J. H.; Orfanou, K.; Driva, P.; Iatrou, H.; Hadjichristidis, N.; Lohse, D. J. *Macromolecules* **2008**, *41*, 9165.